

# Assignment 3

## TTK4190 - Guidance and Control of Vehicles

Shiv Jeet Rai  
Arne Selle  
Erik Liland

17. November 2015

### Contents

|          |   |           |
|----------|---|-----------|
| <b>1</b> | <b>Autopilot design</b>                 | <b>2</b>  |
| 1.1      | Heading autopilot . . . . .             | 2         |
| 1.2      | Speed autopilot . . . . .               | 8         |
| <b>2</b> | <b>Path following and Path tracking</b> | <b>13</b> |
| 2.1      | Path Generation . . . . .               | 13        |
| 2.2      | Path following . . . . .                | 14        |
| 2.3      | Path Tracking . . . . .                 | 15        |

# 1 Autopilot design

## 1.1 Heading autopilot

### Analysis of ship characteristics

To be able to model the ship in a good way we ran many simulations with different rudder angle and measured the steady-state yaw rate. We then made a  $\delta - r$  plot of the result. Since the ship was turning port while giving a positive rudder command, this plot and the rest of the assignment is made with a fixed gain of -1 on  $\delta_c$ .

Figure 1:  $\delta - r$  plot

From figure 1 we clearly see the non-linear characteristics of the ship. Since we only want to control heading and course, a 1-DOF heading model i.e. first- or second order Nomoto model with or without non-linear extensions can be used. To further investigate the effect of the non-linear characteristics of this ship, we compare the actual response with different models at different rudder angles. It should also be noticed that the ship has a constant drift to starboard when  $\delta_c = 0$  as seen by the curve not passing through the origin. We compensate for this through the rest of the modeling part by adding a fixed rudder angle of  $0.52^\circ$  to the rudder input. We only need this correction while estimating the model parameters. In a closed loop, the integral effect will cancel both this drift and drift caused by wind, current and waves.

### 2. order linear Nomoto model

$$\frac{r}{\delta}(s) = \frac{K(1 + T_3s)}{(1 + T_1s)(1 + T_2s)} \quad (1)$$

The second order Nomoto model follows the ships overshoot quite well.

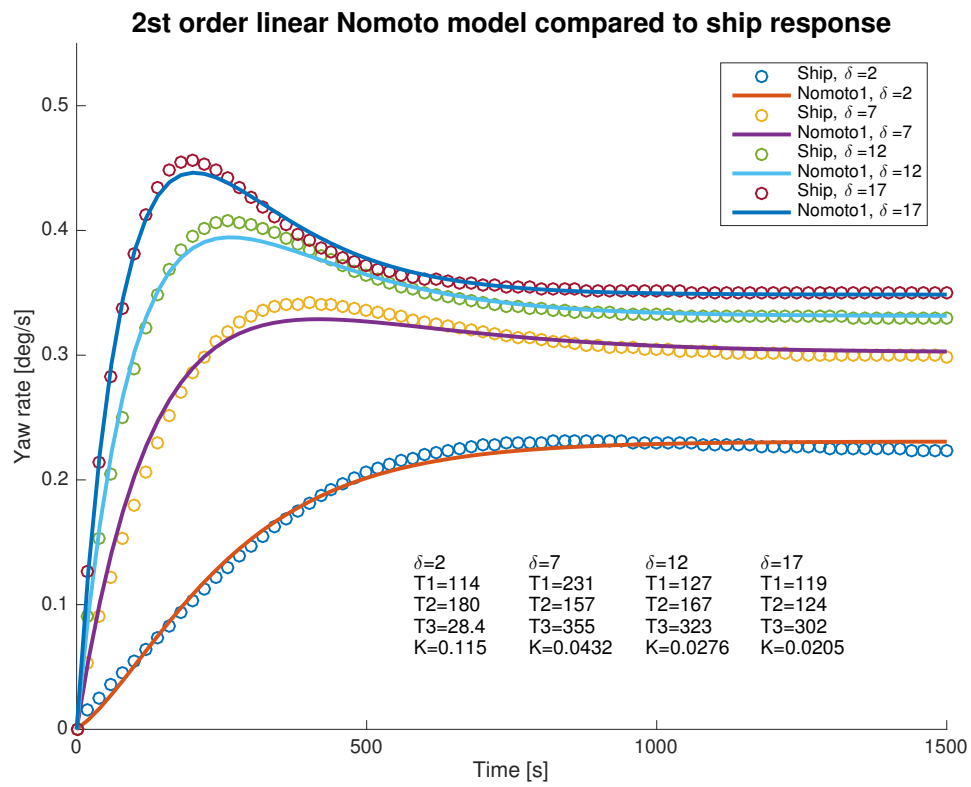


Figure 2: 2.order linear Nomoto model

## 1. order linear Nomoto

$$\frac{r}{\delta}(s) = \frac{K}{(1 + Ts)} \quad (2)$$

We also tried the first order version Nomoto, and as expected the model will only be accurate for small rudder angles, and is therefore not very good for modeling the overshoot and non-linearities.

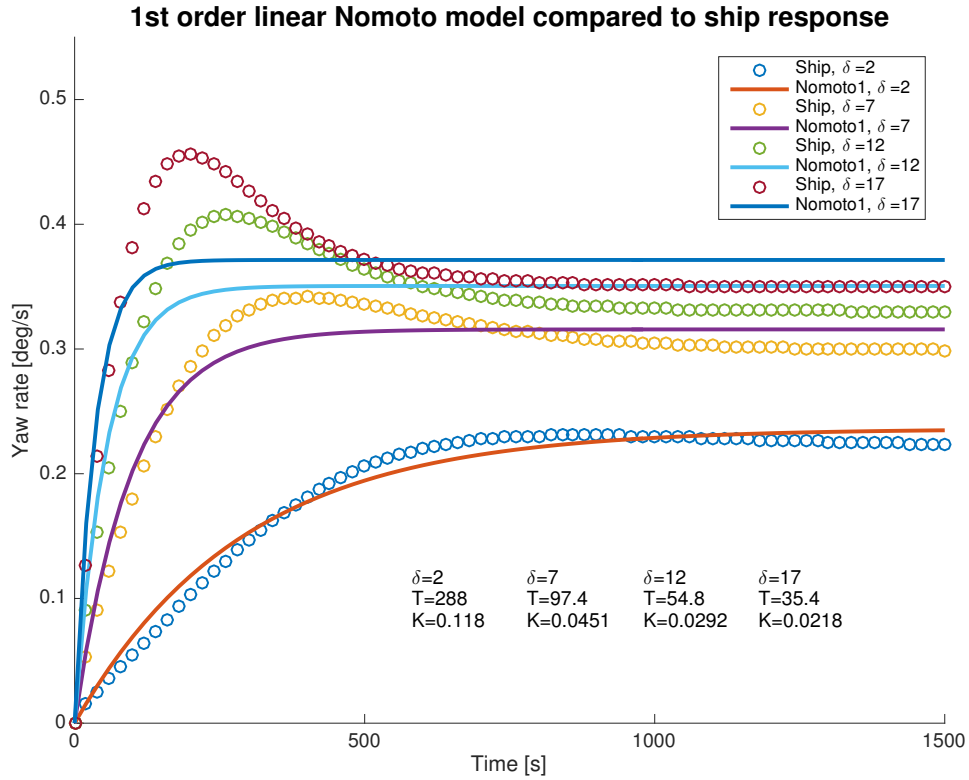


Figure 3: 1.order linear Nomoto model

## 2. order non-linear Nomoto

$$T_1 T_2 \ddot{r} + (T_1 + T_2) \dot{r} + K H_B(r) = K(\delta + T_3 \dot{\delta}) \quad (3)$$

$$H_B(r) = b_3 r^3 + b_2 r^2 + b_1 r + b_0$$

Here the steady state of  $H_B(r) = \delta$ , and  $b_0$  have already been taken care of in the fixed rudder offset, and the assumed symmetry in the hull leads to  $b_2 = 0$ . We then only need the first- and third-order term to describe the maneuvering characteristics. By curve fitting  $H_B(r) = b_3 r^3 + b_1 r = \delta$  to the obtained delta-r curve, we estimate the parameters  $b_3$  and  $b_1$ . We also tried to add a second order term in the equation, and the resulting curve is much better for smaller rudder angles.

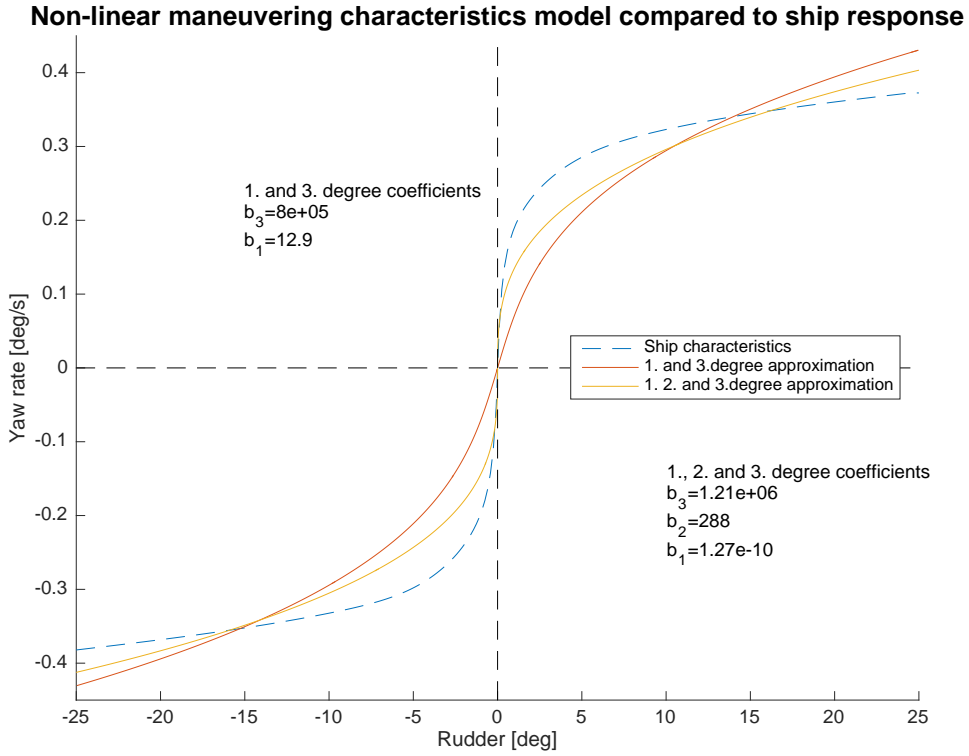


Figure 4: Approximation of ship characteristics

When curve fitting this model to the ship, the errors in the estimated ship characteristics becomes very clear. Since the steady-state is  $b_3 r^3 + b_2 r^2 + b_1 r = \delta$ , and we can see from figure 2 that the only rudder angle where the actual and estimated curves intersect is at about  $\delta = 17^\circ$ , this is the only rudder angle where the steady-state model solution will match the ship as seen in figure 5.

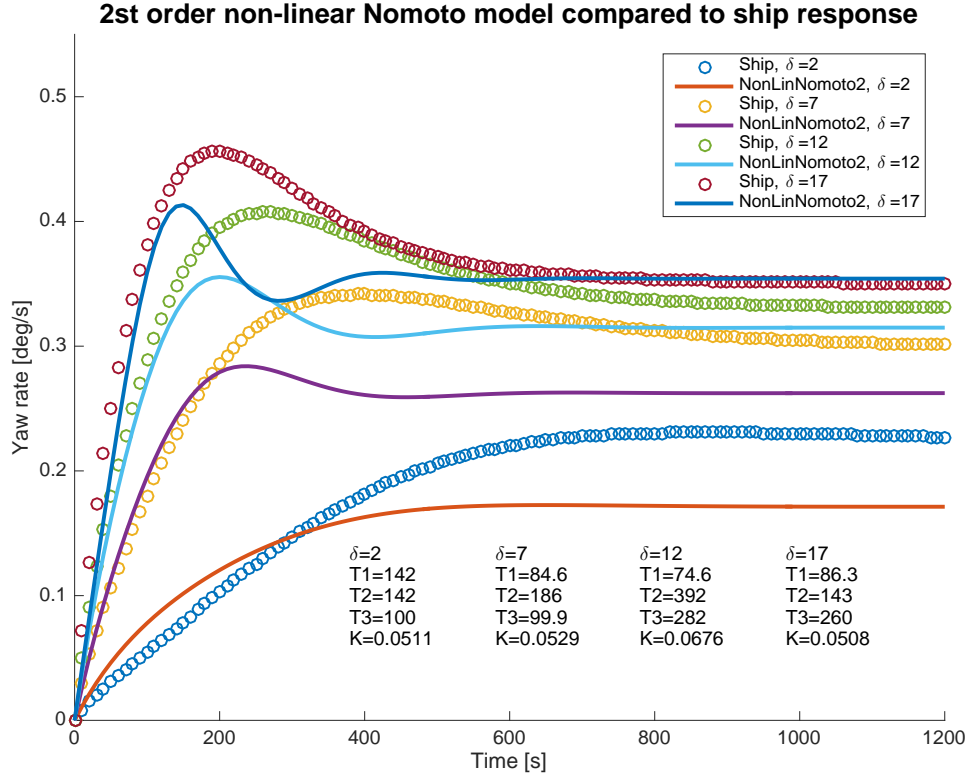


Figure 5: 2.order non-linear Nomoto model

### 1. order non-linear Nomoto

Norbins' extension of the linear first order model:

$$T\dot{r} + H_N(r) = K\delta \quad (4)$$

$$H_N(r) = n_3 r^3 + n_2 r^2 + n_1 r + n_0$$

Where the steady state of  $H_N(r) = K\delta$ . We know from [Fossen, 2011] that  $n_i = \frac{b_i}{|b_1|}$ , and since our ship is stable we know that  $n_1 = 1$ , and  $n_3 = \text{sign}(b_3) = 1$  thus resulting in following model.

$$T\dot{r} + r^3 + r = K\delta \quad (5)$$

When curve fitting this model we got as expected a response which is not able to follow the overshoot to the ship as seen in figure 6.

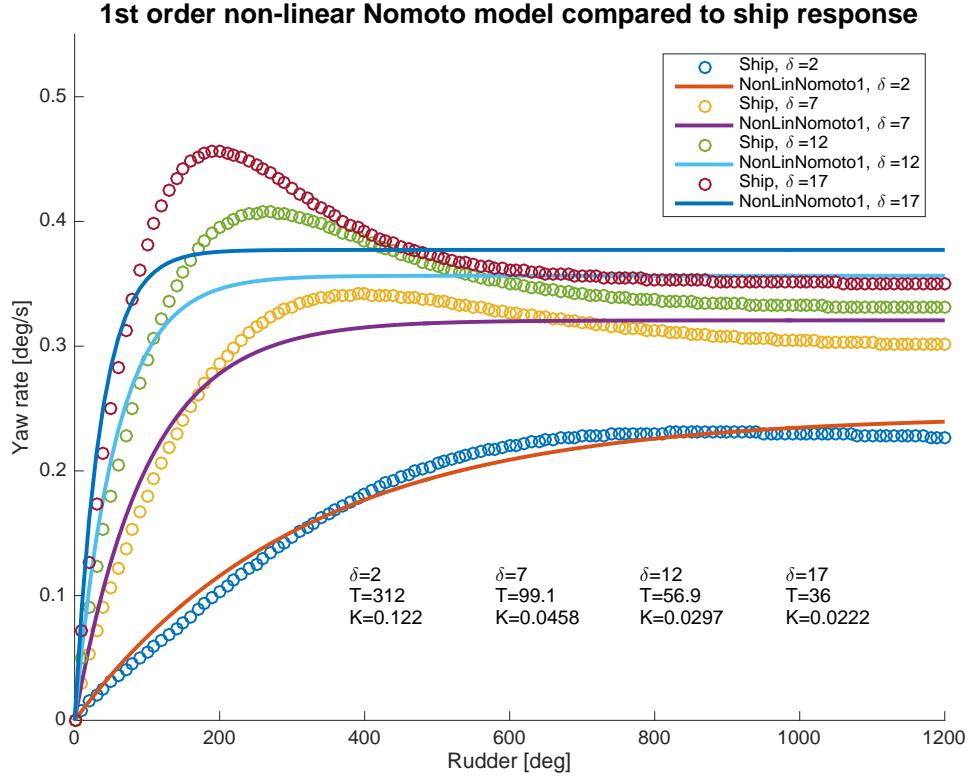


Figure 6: 1.order non-linear Nomoto model

### Heading model conclusion

Both first order models where not able to follow the overshoot and oscillations to the ship, and would therefore make a poor model. The second order model with non-linearities was hard to get good steady-state solution on, and was very hard to do curve fitting on. Which in turns means that the model preformed bad. This leaves us with the second order linear model which where easy to curve-fit to the original response, and preformed quite well. This is the model we are using through the rest of the assignment, with an added integrator for heading.

$$\frac{\psi}{\delta_c}(s) = 0.03 \frac{(1 + 320s)}{s(1 + 130s)(1 + 150s)} \quad (6)$$

### Heading control law

When using a linear model, the obvious choice of controller would be a PID. We have a stable ship under the influence of current, so we need at least a PI-controller. We ended up using this controller.

$$\begin{aligned} \delta_c &= K_p \tilde{\psi} - K_i \int \tilde{\psi} - K_d \tilde{r} + b_0, \\ K_p &= 50, \quad K_i = 0.7, \quad K_d = 350, \quad b_0 = 0.09 \end{aligned} \quad (7)$$

In addition we are filtering  $\psi_d$  with a third order low pass filter to avoid sharp spikes in the derivate part of the controller. We are using pure derivative (s) to avoid phase lag on the derivative compared with the rest of the controller. The bandwidth of the filter is set slightly lower than the maximum bandwidth of the ship.

### Sine wave tracking

From figure 7 we can see that the ship is following the desired heading after a short time, when the initial transient is gone.

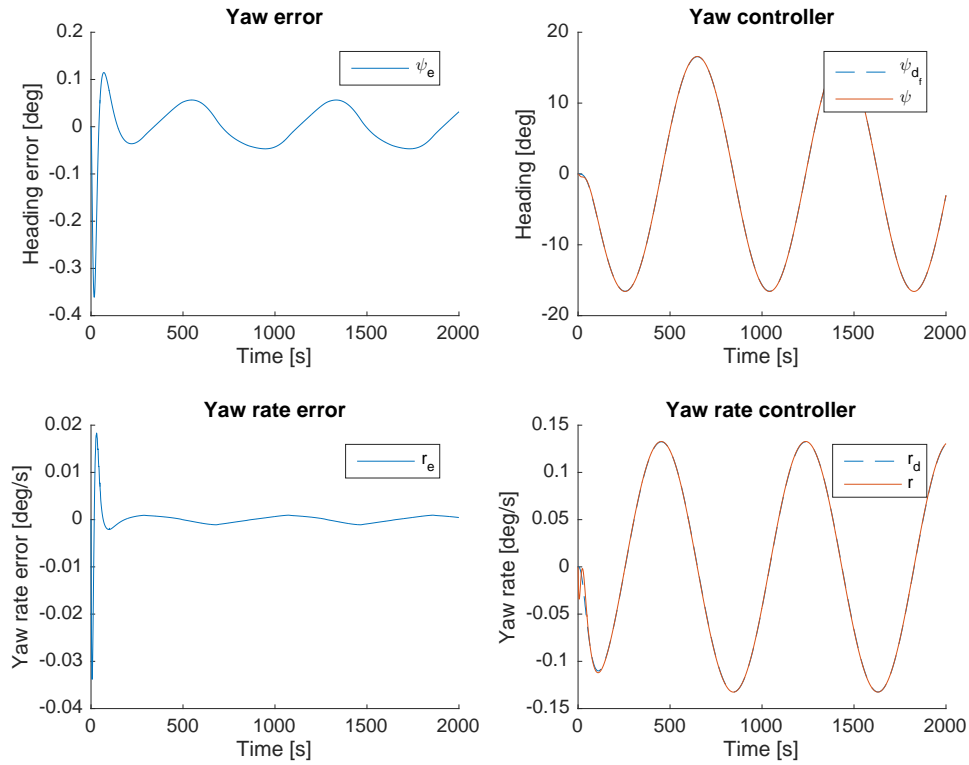


Figure 7: Sine wave tracking

## 1.2 Speed autopilot

We started studying the steady state characteristics of the surge speed as a function of propeller shaft velocity.



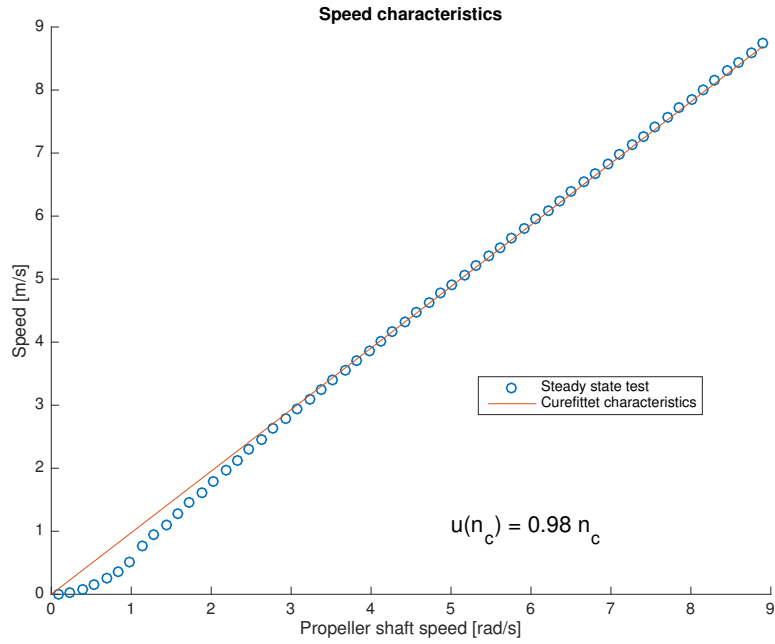


Figure 8: Speed characteristics

As can be seen in figure 8, the characteristics of the ships surge speed is linear. This motivates a first or second order linear surge speed model, where the surge speed is decoupled from the rest of the system. We are assuming

$$u \gg v$$

which leads to:

$$U = u$$

### 1.order linear model

We then try a first order linear model.

$$\frac{u}{n_c}(s) = \frac{K}{1 + Ts} \quad (8)$$

Which gives us a quite good estimate of the speed dynamics (figure 9). Although we have a linear steady state relationship between shaft and surge speed, the time constant varies. This is a sign of a non-linear effect like quadratic damping.

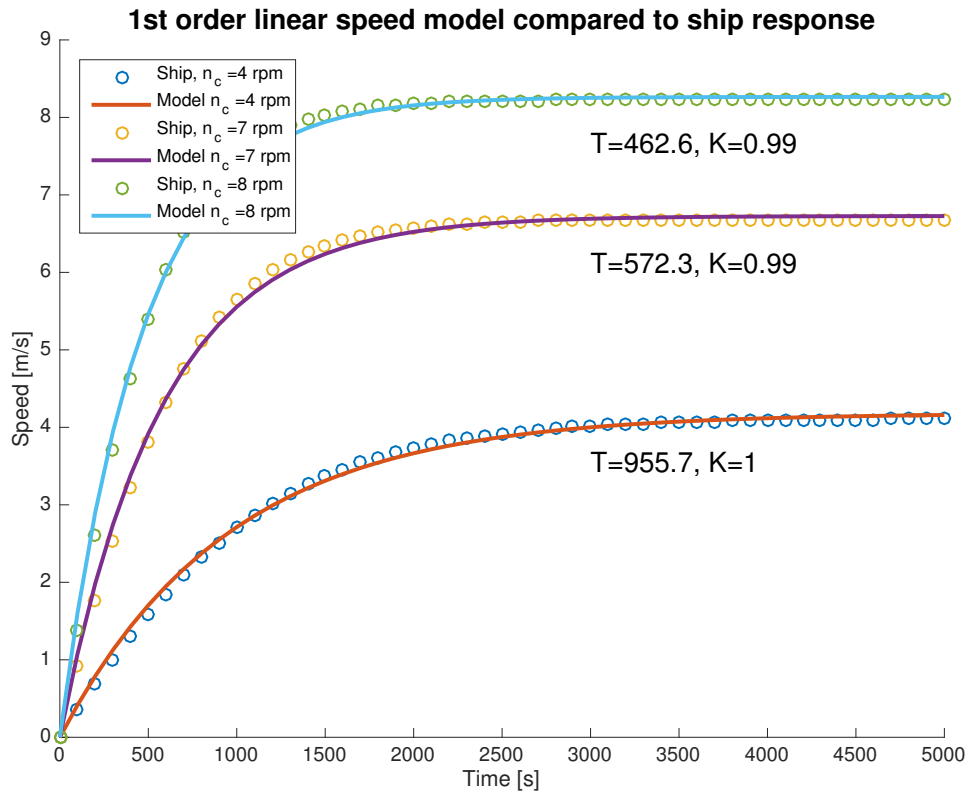


Figure 9: 1.order linear speed model

### 1.order quadratic model

We also tried a quadratic model.

$$\dot{u} = \frac{n_c - K}{K_1|u|u - K_2u} \quad (9)$$

Which gave a slightly better curve fit.

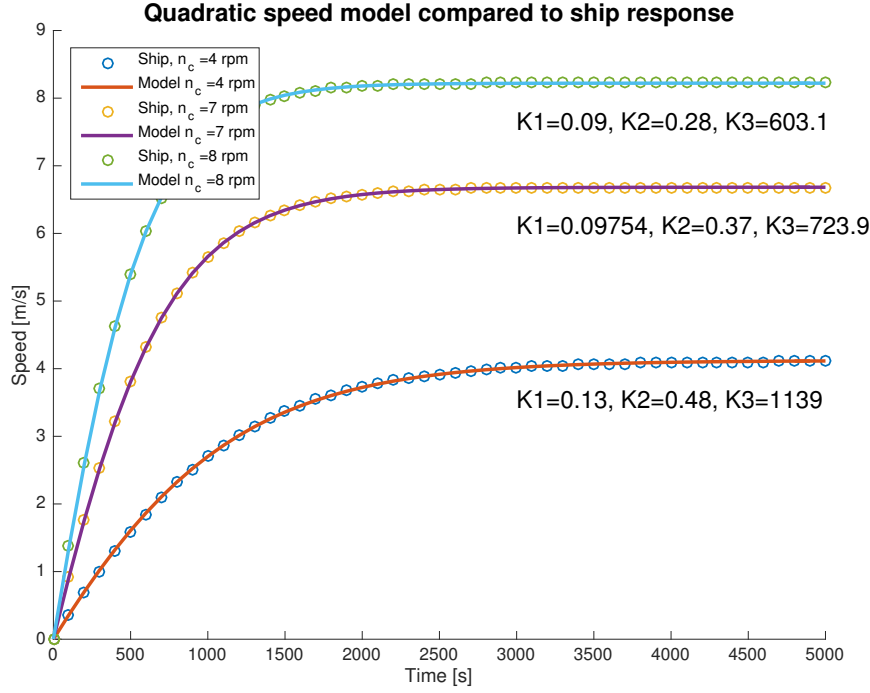


Figure 10: 1.order quadratic speed model

### Speed model conclusion

Both the linear and quadratic model were able to follow the ship's response quite well. The quadratic is closer to reality, and will therefore be better when you need a more accurate model. For simpler analysis and controller, the linear model will do just fine.

### Controller

The surge dynamics are stable and a PI controller will be able to reduce  $\tilde{u}$  to zero. To improve the response of the controller, we added a force feed forward with the same gain as the steady state response. We then added a feedback PI-controller with anti-wind-up on the integral effect to take care of disturbances and modeling errors. The complete controller structure is shown in equation 10. We also low pass filtered  $u_d$  to avoid too fast changes in the speed reference. As in the heading controller, the LPF was set to slightly slower than the bandwidth of the surge dynamics.

$$n_c = K_{ff}u_d - K_p\tilde{u} - K_i \int \tilde{u} \quad (10)$$

### Step response

The step response can be seen in figure 11.

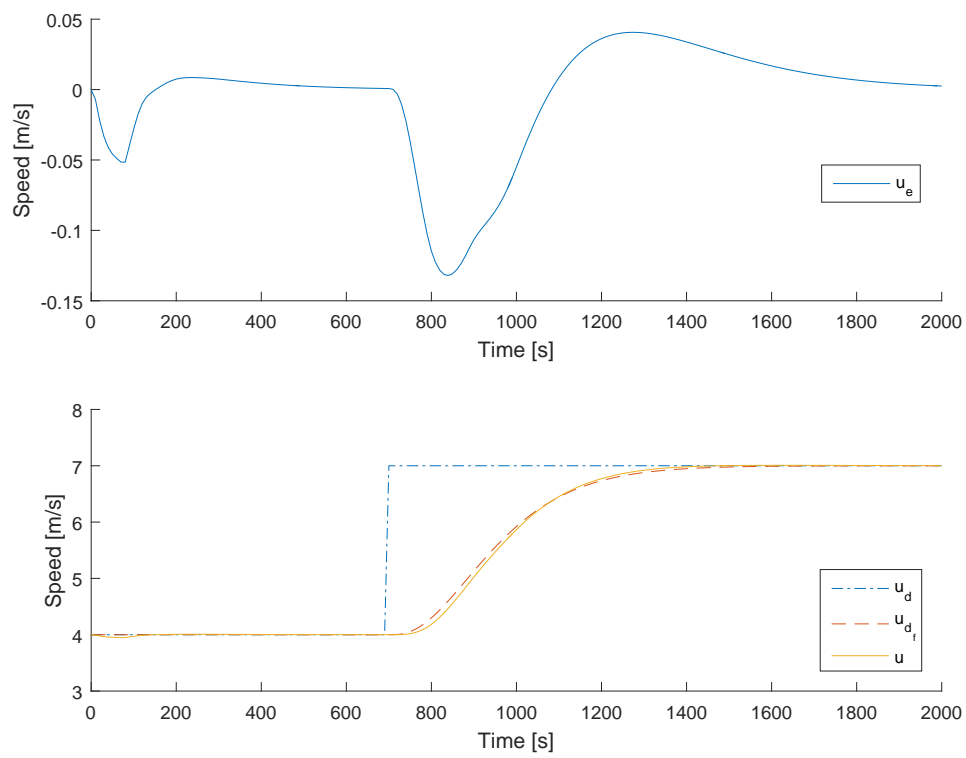


Figure 11: Speed step response

## 2 Path following and Path tracking

### 2.1 Path Generation

We can see from figure 12 that both methods based on continuous interpolation ("Piecewise Cubic Hermite Interpolating Polynomial" and "Cubic spline data interpolation") are very smooth, but they are more off-track than on-track. The piece-wise continuous interpolation are the crudest method of them all, since it in no way takes in to consideration the dynamics of the ship. The combination of circles and straight lines may look like the obvious best solution, but it does have a step in yaw rate ( $r$ ), which means that the ship will not be able to follow the circle exactly while turning. Beside that, the lines and circles makes an excellent path for a ship to follow since it reduces the amount of time the ships actively uses its rudder, and therefore minimizes the drag on the ship. The turning radius set in the last method would be selected equal or larger to the ships turning radius. Preferably set it large enough to not loose to much speed, and small enough to not collide with someone/something. The nice about these turning radius, is that they can be adapted to the situation.

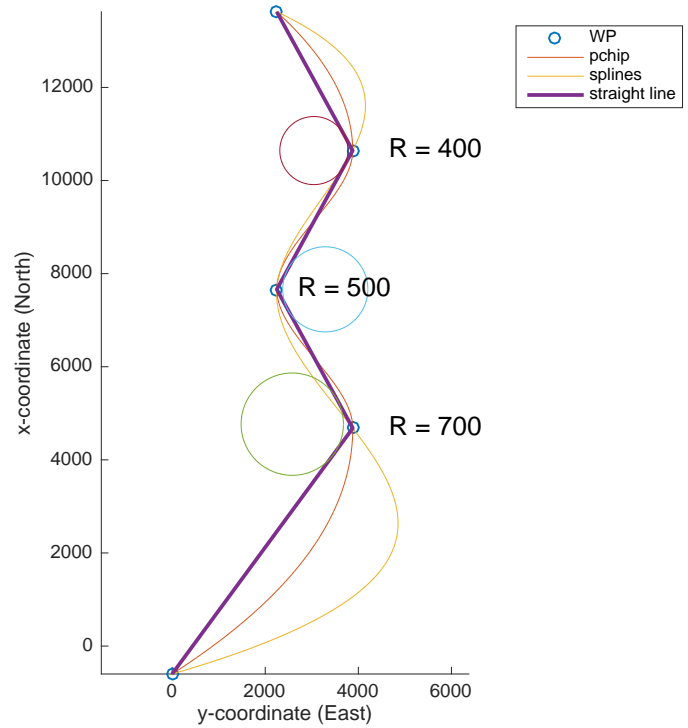


Figure 12: Different trajectories

## 2.2 Path following

Figure 13: Path following

We implemented a lookahead-based steering law, based on figure (10.10) in [Fossen, 2011], which kinematically guarantee path following. The desired course  $\chi_d$  is made up of two parts, a path-angle  $\chi_p$  and a cross-track error correction  $\chi_r$ . The cross-track error correction is essentially a PI-controller, normalized with an inverse tangent. The proportional gain is the inverse of the lookahead distance  $\Delta_s$  which is a design parameter.

$$K_p = \frac{1}{\Delta_s} \quad (11)$$

The integral effect of the controller is quite complex, since we only want the integrator to compensate for small slow-changing disturbances like wind and current when the ship has come to a near steady state. To achieve this, we made an integral structure that takes into consideration the yaw rate of the ship  $r$ , the cross-track error  $e$ , a soft maximum integral effect and an anti-wind-up corrector and a regular gain on the end result. The total control law is listed in equation 12.

$$\begin{aligned} \chi_d &= \chi_p + \chi_r \\ \chi_r &= \text{atan}(P - I) \\ P &= K_p e \\ I &= \int K_i e_i \\ e_i &= \begin{cases} 0, & \text{if } |r| > r_{lim} \text{ or } |e| > e_{lim} \\ \frac{e}{k_1 + k_2 \frac{|I|}{I_{max}}}, & \text{if } (I > I_{max} \text{ and } e > 0) \text{ or } (I < -I_{max} \text{ and } e < 0) \end{cases} \end{aligned} \quad (12)$$

From the cross-track error (figure 14) it can be seen that when the ship first get aligned and on the track, the error stays within  $\pm 200\text{m}$ .

Figure 14: Cross-track error

### 2.3 Path Tracking

Figure 15: Target tracking (zoom)

We want to follow a target with constant speed and course made up by the two first waypoints. This is essentially the same as path following with only one active segment, and a speed controller ensuring that we intercept the target and keep a constant distance from it. The heading and speed controller in use is the same as in section 2.2, and we have added a computation of  $\tilde{\mathbf{p}} = \mathbf{p} - \mathbf{p}_t$  which is a two dimensional vector from the target to our position. This vector is used by the speed guidance block to determine the distance to the target, and calculate the desired speed vector.

$$\begin{aligned} \mathbf{v}_d &= \mathbf{v}_t + \mathbf{v}_a \\ \mathbf{v}_a &= -\kappa \frac{\tilde{\mathbf{p}}}{\|\tilde{\mathbf{p}}\|} \\ \kappa &= U_{a,max} \frac{\|\tilde{\mathbf{p}}\|}{\sqrt{(\tilde{\mathbf{p}})^T \tilde{\mathbf{p}} + \Delta_s^2}} \end{aligned} \tag{13}$$

Where  $U_{a,max}$  and  $\Delta_s^2$  are design parameters describing the maximum relative velocity between the intercepting ship and target and transient interceptor-target rendezvous behavior respectively.

Figure 16: Target tracking

Figure 17: Interception of target

## References

[Fossen, 2011] Fossen, T. I. (2011). *Handbook of Marine Craft Hydrodynamics and Motion Control*. John Wiley & Sons, West Sussex, United Kingdom.